A ROLE FOR DIACYLGLYCEROL KINASE γ IN TRAFFICKING OUT OF THE *trans* GOLGI NETWORK

A Thesis

Presented to the Faculty of the Graduate School

of Cornell University

in Partial Fulfillment of the Requirements for the Degree of

Master of Science

By

Kevin Dean Thorsen

December 2017

ABSTRACT

The formation of cargo carriers in the secretory pathway occurs primarily through the action of coat proteins (i.e. COPI, COPII and clathrin coats). However, a subset of cargo carriers, primarily membrane tubules, form independently of coat proteins in a process that remains poorly understood. In an siRNA screen of the human kinome, our lab identified diacylglycerol kinase γ (DGKγ) as important in the generation of coat-independent tubular cargo carriers at the Golgi complex and *trans* Golgi Network (TGN). DGKs converts diacylglycerol (DAG) into phosphatidic acid (PA). Both DAG and PA are signaling lipids known to regulate different steps in trafficking at the Golgi, and a role for DGKs has been anticipated but remains unclear. Here we show that drug- or siRNA-mediated inhibition of DGKγ reduced delivery of a subset of cargoes to the plasma membrane. Inhibition of DGKγ also caused fragmentation of the Golgi complex, a characteristic phenotype of inhibitors of intra Golgi trafficking, as Golgi structure homeostasis depends on continuous membrane tubule formation between cisternae. Furthermore, we found a novel interaction of DGKγ with the regulatory and catalytic subunits of PPP6, as well as the Rab GEF, DENND4C, both of which contribute to trafficking out of the Golgi and may thus suggest a mechanism for DGKγ in this process. Our findings implicate DGKγ as a regulator of trafficking at the Golgi and TGN via a novel role in tubule formation, with several compelling mechanistic possibilities to unravel.

BIOGRAPHICAL SKETCH

Kevin Thorsen was born in Glasgow, Montana, on February 12, 1988, the youngest of four sons of Carmen and Michael Thorsen. He attended Our Lady of Lourdes Catholic School from kindergarten through 8th grade and Charles M. Russell Public High School, both in Great Falls, Montana. In 2006, he entered the University of Montana and was awarded Bachelor of Arts degrees in French Linguistics, Psychology, and Human Biology in 2011. He then worked as a research technician in the Department of Biological Sciences, University of Montana, in Dr. Jesse Hay's lab. In 2014 he entered the Graduate School of Cornell University as a student in Biochemistry, Molecular and Cell Biology.

ACKNOWLEDGEMENTS

I am most grateful to my mentor, Professor William J. Brown. This project was started by Kevin Ha, and the focus on DGKγ was chosen based on important preliminary work by Catalina Pereira and Carolyn Kelly. I would also like to acknowledge and thank undergraduates Lisa Velez-Velez, Zachary Kassir, Helen He, and Raymond Gui, who worked with me on this project and others. I would also like to thank Jaclyn Beckinghausen, Alex Henkel, and Jennifer Roscoe for helping to keep the lab running and for troubleshooting protocols; much of this work depended on it. This work was supported by NIH grant GM101027 to WJB and by an NSF Graduate Research Fellowship to KDT.

TABLE OF CONTENTS

LIST OF FIGURES

LIST OF TABLES

LIST OF ABBREVIATIONS

Arf	ADP-ribosylation factor
Brefeldin A	BFA
COP	coatomer protein
CtBP1	C-terminal-binding protein 1
DAG	diacylglycerol
DENND4C	DENN domain containing 4C
DGK	diacylglycerol kinase
ER	endoplasmic reticulum
FBS	fetal bovine serum
GPI	glycosylphosphatidylinositol
GP135	glycoprotein 135
GPP130	Golgi phosphoprotein of 130kDa
LPAT	lysophosphatidyl acyltransferase
MEM	minimum essential media
MS	mass spectroscopy
PA	phosphatidic acid
PAP	phosphatidic acid phosphatase
PBS	phosphate-buffered saline
$PI(4,5)P_2$	Phosphatidylinositol 4,5-bisphosphate
PI4K	Phosphatidylinositol 4-phosphate kinase
PKC	protein kinase C
PLA_2	phospholipase A_2
PLC	phosphoinositide phospholipase C
PM	plasma membrane
PPP2	serine/threonine protein phosphatase 2
PPP6	serine/threonine protein phosphatase 6
RUSH	Retention Using Selective Hooks
SBP	streptavidin-binding peptide

SDS-PAGE	sodium dodecyl sulfate polyacrylamide gel electrophoresis
SILAC	Stable Isotope Labeling with Amino acids in Cell culture
ssHRP	secreted soluble horse radish peroxidase
TEM	transmission electron microscopy
TGN	*trans* Golgi network
TRP	transient receptor potential
VSV-G	vesicular stomatitis virus protein-G

CHAPTER ONE

INTRODUCTION

The trafficking of cellular components within and out of the cell is fundamental to eukaryotic cell biology. It is critical for maintaining necessary compartmentalization of cellular functions and for the exchange of materials between the cell and its environment[1]. Canonically, membrane trafficking occurs via vesicles, coated or uncoated[2]. However, the formation of cargo carriers for transport from the trans-Golgi Network (TGN) to the plasma membrane (PM) remains unclear and appears to involve several kinds of cargo carriers. Some cargoes are trafficked from the TGN in clathrin-coated vesicles, and these can either travel directly to the PM or first go to endosomes and from there use endosomal recycling pathways to get to the PM[3, 4]. However, another subset of cargo uses tubular cargo carriers that form independently of coat proteins[5]. How these membrane tubules form without coat proteins remains unclear.

We performed a screen for genes involved in membrane tubule formation using the fungal metabolite Brefeldin A (BFA), which inhibits the fission of tubules from the Golgi and thus is thought to exaggerate normally-occurring tubule formation[6]. The screen identified several members of the diacylglycerol kinase (DGK) family as positive regulators of membrane tubule formation. DGKs convert diacylglycerol (DAG) into phosphatidic acid (PA), one step in a network of lipid metabolism (Figure 1). Compellingly, DAG and PA are known to be involved in several steps in secretion [7-13]. Both PA and DAG act as lipid messengers in numerous signaling pathways, both have been shown to regulate trafficking machinery at the Golgi, and because of their conical shape, they are both thought to facilitate the membrane bending and fusion that occur during the life cycles of vesicles and tubules[9]. At the TGN, the roles of DAG and PA remain unclear. One study has shown that depleting DAG via enhanced DGK activity inhibits

recruitment of trafficking machinery to the TGN and reduces TGN-to-PM transport, suggesting a negative role for DGK at this step[8, 10-12]. However, a separate study showed that elevating PA via DGK *increases* transport from the TGN *in vitro*[13].

DGKs are present in bacteria, yeast, plants, and animals[14-16]. Yeast have a single DGK, which uses CTP rather than ATP and appears to be involved in vacuolar fission[17]. Mammals have 10 DGK isoforms with conserved kinase and DAG-binding (C1) domains, and these are classified into 5 types based on additional shared structural domains (Figure 2)[18]. These DGK isoforms have varying levels of expression in different tissues, varying localizations, and varying functions[18] (Table 1). Indeed, even among structurally-similar isoforms, there are instances where two isoforms have opposite effects on the same process, such as in the positive and negative regulation of macrophage differentiation of leukemia cells by DGKα and DGKγ, respectively[19]. Increasing evidence suggests that DGKs are involved in several membrane trafficking events, including clathrin-mediated and clathrin-independent endocytosis[20], recycling endosome function[21], synaptic transmission[22-24], insulin secretion[25], and trafficking out of the ER[26] (Table 1). Among the DGKs identified in our screen, knockdown of DGKγ showed the strongest inhibition of membrane tubule formation induced by BFA (unpublished data). Here we show that knockdown or drug (R59949) inhibition of DGKγ significantly inhibits the formation of physiological cargo-carrying tubules and inhibits the delivery of a subset of cargoes to the plasma membrane. Specifically, DGKγ knockdown or inhibition slowed the delivery of a soluble secreted horse radish peroxidase (ssHRP), vesicular stomatitis virus protein-G (VSV-G), and GP135 to the plasma membrane, but did not slow delivery of a glycosylphosphatidylinositol (GPI)-anchored protein. This inhibition appears to occur at a post-ER step in trafficking, as ER-to-Golgi trafficking was unaffected. DGKγ knockdown also caused

fragmentation of the Golgi complex, a characteristic phenotype of inhibitors of Golgi trafficking[27]. Finally, using a SILAC-MS approach to identify protein interactors of DGKγ, we found that it interacts with established trafficking proteins DennD4C and PPP6, suggesting a possible mechanism of action for DGKγ in trafficking to the PM. In summary, we provide evidence for a role for DGKγ in constitutive trafficking from the Golgi to the PM, with a discussion of possible mechanisms given below.

CHAPTER TWO

RESULTS

DGKγ contributes to the formation of tubular cargo carriers at the TGN

Using the Retention Using Selective Hooks system[28], which locks a fluorescently-labeled cargo in the ER until the addition of biotin (Figure 3), we investigated the role of DGKγ in the formation of anterograde-cargo-carrying tubules. We found that following the addition of biotin, GP135 was released from the ER and appeared in the Golgi complex after 30 min. GP135 was then seen to exit the TGN primarily in membrane tubules, which travelled to and fused with the PM (Figure 3). First we quantified tubule formation in cells knocked down for DGKγ. Commercial antibodies for endogenous DGKγ failed to detect the protein in a Western blot, so as a measure of the effectiveness of our DGKγ-directed siRNA, we co-transfected EGFP- DGKγ and measured its knockdown using an antibody against GFP .We were able to achieve a >95% knockdown of exogenously-expressed EGFP-DGKγ 48 hours after transfection (Figure 4B). In the RUSH system, we found that membrane tubule formation at the Golgi peaked at 45 min. In siDGKγ cells, tubule formation was inhibited by ~60% (Figure 4A). Similarly, inhibiting DGKγ with R59949, a Type I DGK inhibitor, also reduced tubule formation, in a dosage- and time-dependent manner (Figure 4C-D).

DGKγ contributes to the delivery of a subset of cargoes from the ER to the PM

To assess whether inhibition of membrane tubule formation had a functional impact on delivery of GP135 to the PM, or whether GP135 might as readily travel in vesicles, we next measured the delivery of GP135 to the PM. Again using the RUSH system, we stained cells using an anti-Streptavidin Binding Peptide (SBP, part of the RUSH construct and

luminally/externally exposed) antibody in the absence of permeabilizing agents so that only the GP135 that had reached the PM would be stained (Figure 3A, bottom panels)[28]. We found that in control cells, delivery to the PM peaked at 80 min after releasing the cargo from the ER, and that both siRNA- and drug-mediated inhibition of DGKγ significantly reduced delivery of GP135 to the PM (Figure 5A-B). This effect was again dosage-dependent (Figure 5B). We previously showed that knockdown of DGKγ likewise inhibited the secretion of ssHRP and VSV-G-GFP (unpublished data, Kevin Ha). In contrast, using a GPI-anchored RUSH construct, I found that DGKγ inhibition had no effect on the delivery of GPI-anchored proteins to the PM (Figure 6). Thus, DGKγ positively regulates the trafficking of a subset of cargoes to the PM. This supports previous findings that cargoes leaving the TGN are sorted into distinct classes of carriers requiring their own machinery for formation[5]. It is noteworthy that, using the RUSH system, VSV-G was shown to exit the TGN in tubules, along with transferrin receptor and LAMP1, and that these tubules formed independently of clathrin and its adaptor proteins[29]. Therefore DGKγ's may contribute specifically to the formation and function of coat-independent tubular cargo carriers.

DGKγ does not regulate transport from the ER to the Golgi

The trafficking of GP135 from the ER to the PM requires at least 2 steps: ER-to-Golgi transport and Golgi-to-PM transport. To investigate where DGKγ may function, we again used the RUSH system and measured the delivery of GP135 from the ER to the Golgi. While R59949 had a significant effect on TGN-to-PM transport, it had no effect on ER-to-Golgi transport at 15 min or 30 min (Figure 7). Thus, consistent with a role in the formation of Golgi-derived cargo carriers, DGKγ appears to act at the Golgi-to-PM step in the trafficking of GP135.

DGKγ is required for structural homeostasis of the Golgi complex

To further investigate the role of DGKγ at the Golgi complex, we examined Golgi complex ultrastructure in control and R59949-treated cells immuno-stained with anti-GPP130 antibody (*cis* and *medial* Golgi). R59949 treatment caused a slight but significant increase in Golgi fragmentation (Figure 8A). Because immunofluorescence-based microscopy cannot resolve finer Golgi structure, we next examined the Golgi complex using transmission electron microscopy (TEM). Using TEM, we found a dramatic change in Golgi structure in DGKγ-knockdown cells (Figure 8B): Golgi cisternae were rounder, more fragmented, and less stacked together. There are several possible explanations for this. First, Golgi structure homeostasis depends on intra-Golgi transport mediated by membrane tubules, and DGKγ may be involved in this process. Second, by inhibiting anterograde trafficking out of the Golgi, DGKγ knockdown may cause an imbalance in membrane/cargo flow, leading to swelling of the cisternae and disruption of normal function. A third possibility is that DGKγ knockdown triggers apoptosis, which is known to cause Golgi fragmentation[30, 31]. Indeed, a 2-day knockdown, as used in the experiments described here, significantly reduced cell numbers, although it is unclear whether this is due to apoptosis or stalling of the cell cycle, which DGKγ has been implicated in[32]. More experiments will be needed to examine these possibilities.

DGKγ localization

To understand how DGKγ may be functioning at the Golgi, we next examined its localization. DGKγ has been shown to localize to the PM[19, 33-38], partially to the nucleus[32], the cytoplasm[19, 32-40], and, less commonly, to the Golgi complex[39, 40]. We overexpressed EGFP-DGKγ in HeLa cells and found it to be in the cytoplasm and at the PM (Figure 9A, left panel). It

also appeared to decorate a tubular-reticular structure resembling TGN-derived tubules, but it failed to significantly co-localize with any Golgi or TGN markers, or with GP135-containing tubules in a RUSH experiment (data not shown). Rather, it seems that these structures were lamellipodia or membrane ruffles. This localization has been observed previously, where DGKγ was shown to be a negative regulator of lamellipodia formation when overexpressed[34]. A constitutively-active mutant (Δ1-259) of DGKγ[18] (here called EGFP-DGKγCA) appeared to localize slightly more strongly to the PM, but we were unable to quantify this. Intriguingly, in a very small number of cells (<1% of transfected cells), EGFP-DGKγ localized strongly to the Golgi (Figure 9A, right panel). To see where endogenous DGKγ may localize in HeLa cells, we used a commercial anti-DGKγ antibody and visualized DGKγ staining using immunofluorescence. In over 99% of cells, staining appeared as widely distributed puncta (Figure 9B, left panel), which did not colocalize with markers of lysosomes, endosomes or the TGN (data not shown). However, again, in very rare cases, staining looked like classic ER and Golgi staining (Figure 9B, right panel). Thus DGKγ appears to have a dynamic localization. While DGKγ has been shown to translocate to the PM in response to a wide variety of stimuli[19, 33-38], localization to the Golgi has not been linked to any stimuli. We attempted to induce DGKγ to localize to the Golgi using a RUSH experiment (perhaps forcing it onto the Golgi by loading a large bolus of cargo into the Golgi), BFA treatment (which exaggerates membrane tubule formation at the Golgi and thus may recruit tubule forming machinery), propranolol treatment (a phosphatidic acid phosphatase (PAP) inhibitor, which increases PA levels at the Golgi, and therefore may recruit DGKγ through DGKγ's PA-binding ability), and R59949 treatment followed by washout (which may elevate levels of its substrate, DAG, and induce translocation). However, none of these seemed to trigger translocation to the Golgi (data not shown). Therefore,

while DGKγ appears to predominantly localize to the cytoplasm and PM, it may localize at low, normally-undetectable levels at the Golgi, and may, rarely, translocate to the Golgi in response to unknown stimuli. Further experiments are needed to understand its localization and what it may mean for its mechanism of action in trafficking out of the Golgi.

DGKγ interacting proteins

DGKγ has been shown to interact with β-chimaerin (a Rac-GAP)[41] and protein kinase C-γ (PKCγ)[42]. PKCγ has been shown to regulate ER-to-Golgi transport and Golgi-to-PM transport[43], supporting a role for DGKγ in membrane trafficking as well as suggesting a possible mechanism. To uncover more protein interactors for DGKγ, we performed a Stable Isotope Labeling with Amino acids in Cell culture (SILAC)-based mass spectrometry experiment using EGFP- DGKγ and EGFP- DGKγCA as bait, along with EGFP as a control. We used the CA construct of DGKγ to identify interacting proteins relevant to DGKγ in its active state. However, the wild type and CA mutant had remarkably similar sets of protein interactors, with no novel or clearly increased interactions for the CA mutant. With that said, there were several interacting proteins that are known players in membrane trafficking, including several subunits of serine/threonine protein phosphatase 6 (PPP6)[44] and DENN domain containing protein 4C (DENND4C), a GEF for Rab10[45]. These were among the strongest interacting proteins for both wild type and DGKγ-CA, supporting its role in membrane trafficking. Potential mechanisms of action involving these two proteins are discussed below.

CHAPTER THREE

DISCUSSION

How cargo carriers form independently of coat proteins is still largely unclear. Protein kinase D (PKD)[8], phospholipase A_2 (PLA_2)[46-48], lysophosphatidic acid transferases (LPATs)[49], CtBP/Bars[50], and 14-3-3γ[50], among other proteins, seem to be important factors in membrane reshaping leading to initial tubule formation and eventual fission from the Golgi membrane. Potential mechanisms for shaping the membrane into a tubule include the oligomerization of curved proteins around the membrane, extrusion of membranes along cytoskeletal elements, protein insertion into bilayer leaflets, and changes in lipid shape to favor curvature[51]. Among these possible mechanisms, there is evidence to support 3 potentially overlapping mechanisms of action of the DGKs: 1) DAG or PA act as lipid signals to activate or recruit trafficking machinery; 2) DAG and PA promote membrane shaping due to their conical shape and fusogenic properties; and 3) DGKs themselves act as scaffolds to recruit trafficking machinery to specific sites.

DAG and PA as lipid signals for tubule-forming machinery

Many growth factors, neurotransmitters, and other extracellular signals cause a transient rise in DAG levels through the action of phospholipase C (PLC), which hydrolyzes $PI(4,5)P_2$ to create the signaling molecules DAG and IP_3. DAG may also be produced through other metabolic pathways (Figure 2), including sphingomyelin synthase and phosphatidic acid phosphatases. DAG participates in various cellular responses, including cell proliferation, differentiation, and cytoskeletal organization through activation of target proteins[35, 52, 53]. DAG has been shown to recruit/activate membrane trafficking machinery at various points in the

secretory pathway, including Arf GAPs (required in early stages of tubule formation)[54], PKD[8] and PKCh (both required for fission)[55, 56], the synaptic vesicle priming protein UNC-13[57, 58], and Rab3 (required for fusion of secretory vesicles with the PM)[59]. It may also activate Trp channels at the PM, activating Ca^{2+} signaling that may be relevant to trafficking events[60], and it may regulate the activity of several Rho and Ras proteins, which are involved in cytoskeletal reorganization[61] and thus may contribute to membrane shaping involved in membrane tubule formation. DAG has also been shown to induce the antigen-activated exocytosis involved in degranulation of mast cells by activating and inhibiting, respectively, Ras guanyl nucleotide-releasing proteins (RasGRP)[62] and the Orai1 calcium channel[63]. Indeed DGKγ has been implicated in this pathway, as knockdown or DGK antagonists inhibited mast cell degranulation in response to antigen stimulation[39]. Finally, DAG also regulates the secretion of insulin in response to glucose by modulating Munc13, a protein involved in vesicle maturation and exocytosis[25]. In this case, too, DGKγ knockdown inhibited evoked exocytosis.

However, in both insulin secretion and mast cell degranulation, it can be difficult to determine whether DGKγ is regulating DAG or PA pools, as PA and DAG are both needed for evoked exocytosis[64, 65]. In the case of mast cell degranulation, PA regulates PI(4)P5K and sphingosine kinase, which are important for mast cell degranulation[66]. In other cases in membrane trafficking, PA has been shown to be necessary for the recruitment of tubule-forming proteins MICAL-L1 and Syndapin2 to tubular recycling endosomes[67], and DGKα enzymatic activity is specifically required for this[21]. PA also binds the tubule forming protein, dynamin[68] and is a potent stimulator of dynamin's tubule forming activity on liposomes[69]. PA has also been shown to recruit Rab coupling protein (RCP) and thereby promote endosomal recycling of a5b1 integrin[70]. Finally, PA is an intermediate in PtdIns cycling, a fundamental regulator of

membrane trafficking and Golgi function[71]. In support of this, DGK expression appears to reduce TGN levels of PI4P[72], which promotes transport out of the TGN and again, contrary to ours and others' findings, suggests that DGK may act as a negative regulator of TGN-to-PM trafficking.

DAG and PA in membrane shaping

The shape of DAG and PA can vary from cylindrical to conical. As conical lipids, DAG or PA can be aggregated together in one leaflet of a bilayer to induce negative curvature. Negative curvature is thought to drive membrane fission, and both DAG and PA are thought to promote fission in different contexts[73, 74]. In the case of DAG, the degree to which it is conical depends on acyl chain length and degree of unsaturation[75], while for PA it depends on Ca^{2+} levels[76]. There is evidence that under normal cytosolic conditions, PA adopts a cylindrical shape, but at the elevated Ca^{2+} and mildly acidic TGN, it adopts a conical shape[74]. Thus, depending on the shape of DAG, the conversion of DAG to PA in the context of the TGN may act as a molecular switch to promote curvature. This may be the mechanism of fission of tubules at the TGN, where the generation of a high level of phosphatidic acid that leads to fission[77]. On the other hand, the early stages of tubule formation require a combination of positive and negative membrane curvature in the inner and outer leaflet, which varies between different regions of the tubule, i.e. the neck or tip. Because DAG lacks a charged head group, it can flip between leaflets within seconds[78] and thus can possibly contribute negative curvature as needed in different leaflets. This may be directed by natural segregation into appropriately-shaped gaps during membrane extrusion/shaping by proteins. Thus, DAG may be ideal for early stages in membrane tubule formation, which require dynamic combinations of positive and negative

curvature. PA, on the other hand, represents a more rigid curve-inducing presence in a leaflet, as it flips between leaflets at a much slower rate of minutes to hours[78]. In fact, DAG appears to be necessary for the initial formation of membrane buds, while PA and PA-producing proteins appear to act in late stages of membrane tubule formation, leading to membrane fission by generating strong negative curvature in the cytosolic leaflet at the neck of the tubule[9]. In summary, DAG appears to be required in early stages of membrane tubule formation, after which DGKγ may be recruited to form PA, which in turn promotes fission of the tubule form the Golgi. DGKγ may concurrently recruit machinery needed for tubule/vesicle maturation, as described below.

DGK as scaffold

DGK itself has been shown to recruit trafficking machinery to functional sites. In a synergistic recruitment, DGKα and its product PA bind to MICAL-L1 at tubular recycling endosomes, suggesting a positive feedback loop driving tubule formation[21]. Similarly, SNX7 requires binding to DGKζ for localization to sorting endosomes in Jurkat T cells, but in this case DGKζ acts as a negative regulator, as a knockdown accelerates recycling of transferrin from endosomes to PM[79]. In support of a DGK-specific rather than PA/DAG-specific function in trafficking, overexpression of an active *or* kinase dead mutant of DGKδ inhibits formation of COPII vesicles and ER-to-Golgi trafficking of VSV-G[26]. Here we report that DGKγ binds two established regulators of membrane trafficking: PPP6 and DENND4C. PPP6 has been shown to regulate ER-to-Golgi trafficking by dephosphorylating Sec31[44]. While this offers no direct mechanism for DGKγ's function in TGN-to-PM trafficking, PPP6 may similarly regulate an unidentified protein involved in TGN-to-PM trafficking. In contrast, DENND4C is known to

localize to Golgi-to-PM cargo carriers and acts a GEF activating Rab10[45]. Rab10 is involved in the maturation of cargo carriers at the Golgi and eventual fusion with the PM[81, 82]. This interaction, in combination with the DAG/PA- mediated mechanisms described above, suggest that DGKγ may localize to Golgi membrane tubules later in their life cycle to convert DAG to PA, leading to fission from the Golgi, while simultaneously recruiting DENND4C for activation of Rab10 to lead the nascent cargo carrier down its life cycle towards eventual fusion with the PM (Figure 10).

In summary, here I report the involvement of DGKγ in the formation of TGN-to-PM cargo carriers, delivery of GP135, VSV-G, and ssHRP to the PM, and Golgi structure homeostasis, with PPP6 and DENND4C as possible functional interactors.

CHAPTER FOUR

FIGURES

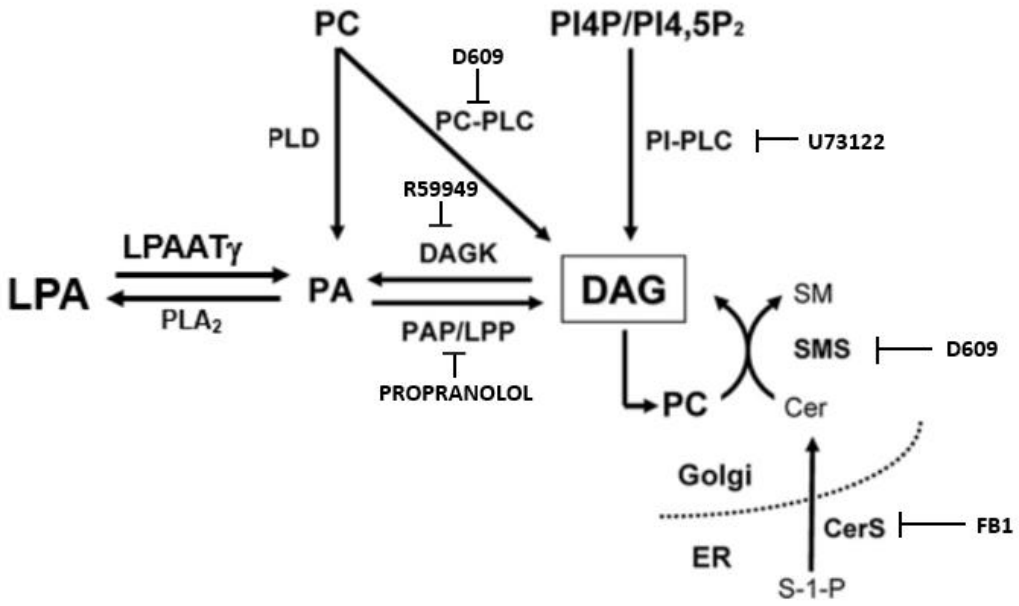

Figure 1. Lipid metabolism pathways associated with DGK. Inhibitors of particular enzymatic reactions are shown.

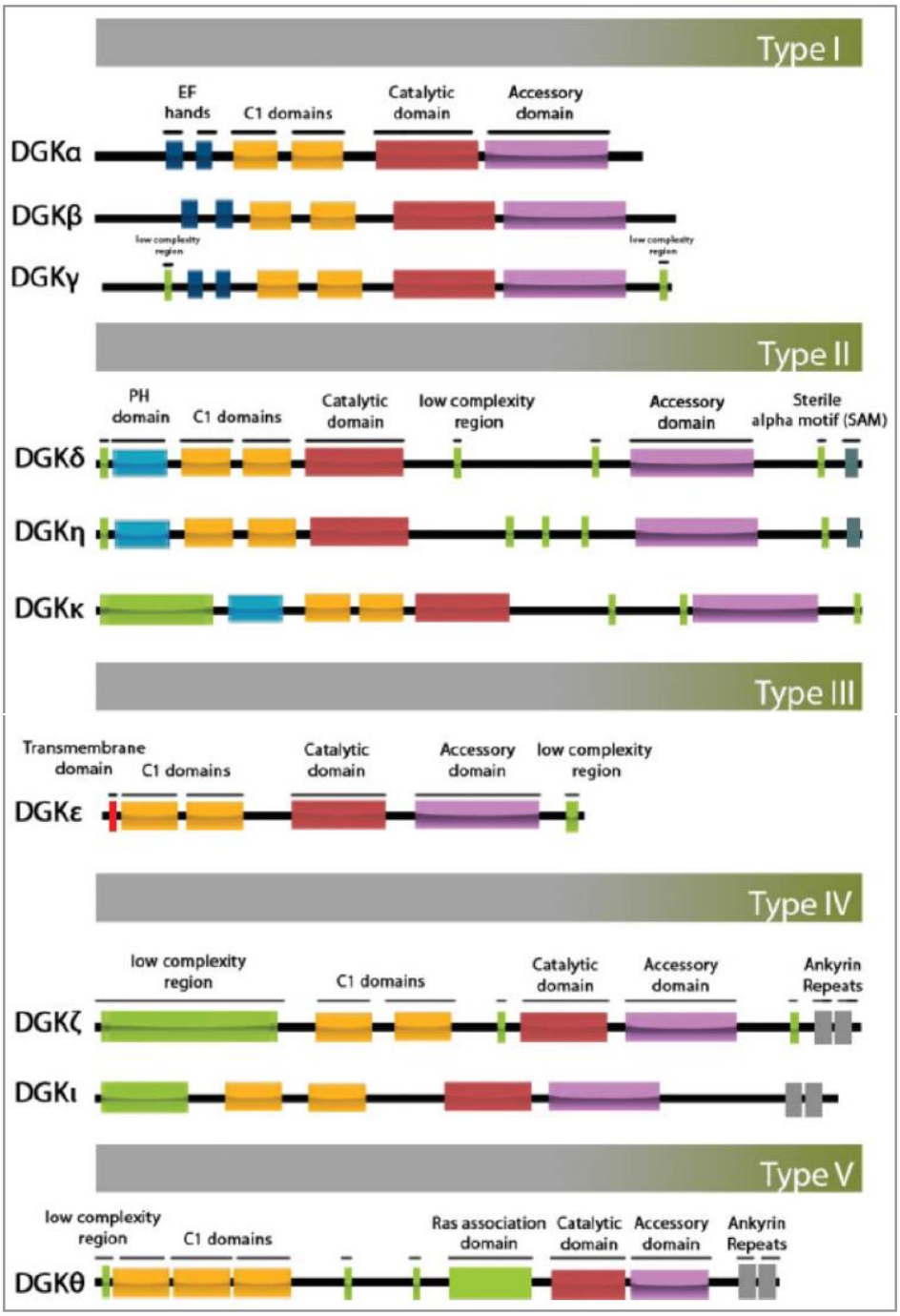

Figure 2. Mammalian diacylglycerol kinases (DGKs). Ten mammalian isozymes are divided into five types based on shared structural domains (from Xie et al. 2015).

Figure 3. RUSH timecourse and Sholl analysis of tubule formation. A) Timecourse of a RUSH experiment. At 0 min, before the addition of biotin, all of the GP135-GFP is in the ER, and there is no surface staining (red channel). By 40 min, cargo has reached the surface and can be detected by surface staining. GP135 exits the TGN via membrane tubules (40min); tubule formation was found to peak at 45 min. Cargo delivery to the surface peaks at 80 min. (B) A cell from a RUSH experiment fixed at 45 min. Sholl analysis[89] was performed by drawing concentric circles around the Golgi and measuring the number of intersections between the drawn circles and fluorescently-labelled membrane tubules. (C) A plot of the number of intersections with membrane tubules at increasing radii. The area under the curve of this plot was taken as a quantification of total tubule length.

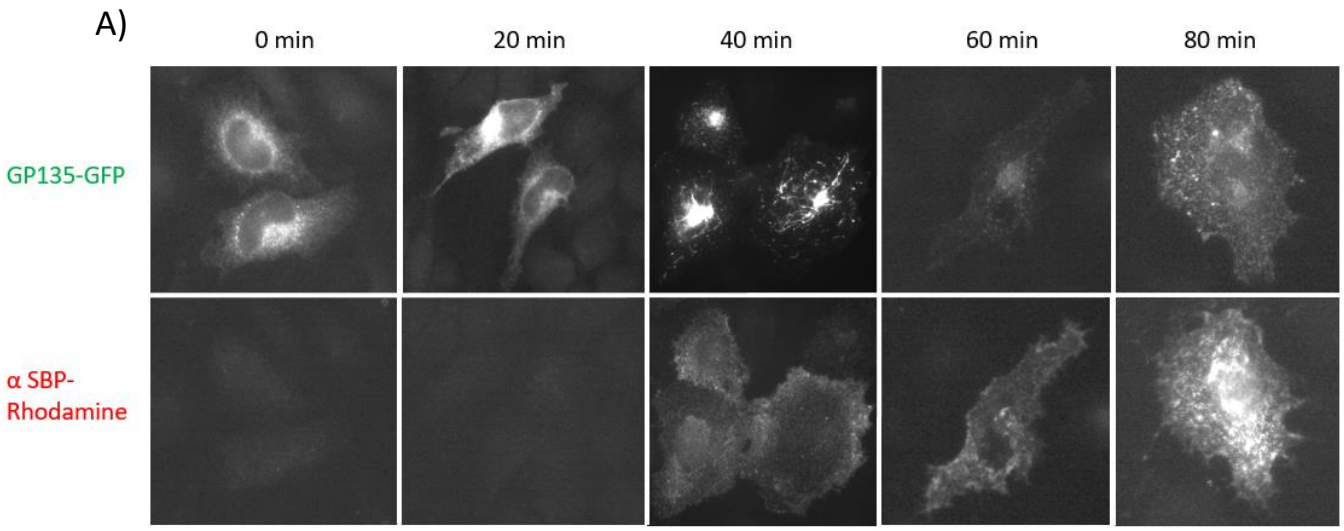
A)
0 min
20 min
40 min
60 min
80 min
GP135-GFP
α SBP-
Rhodamine

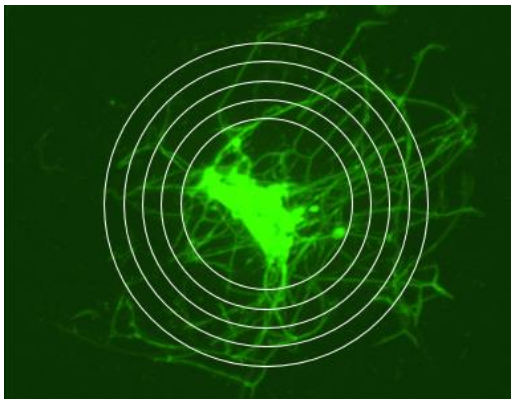
B)

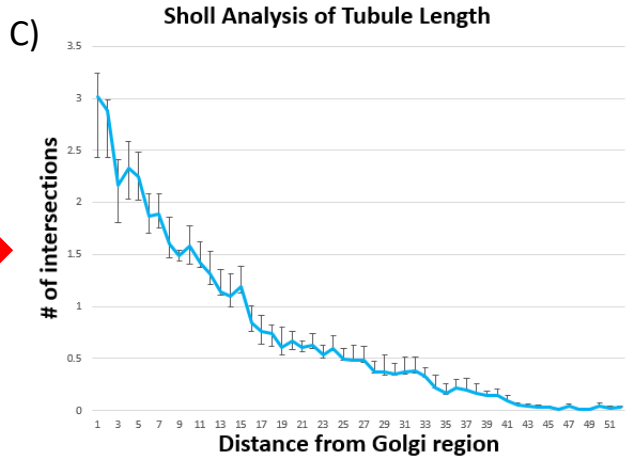
C)
Sholl Analysis of Tubule Length
# of intersections
Distance from Golgi region

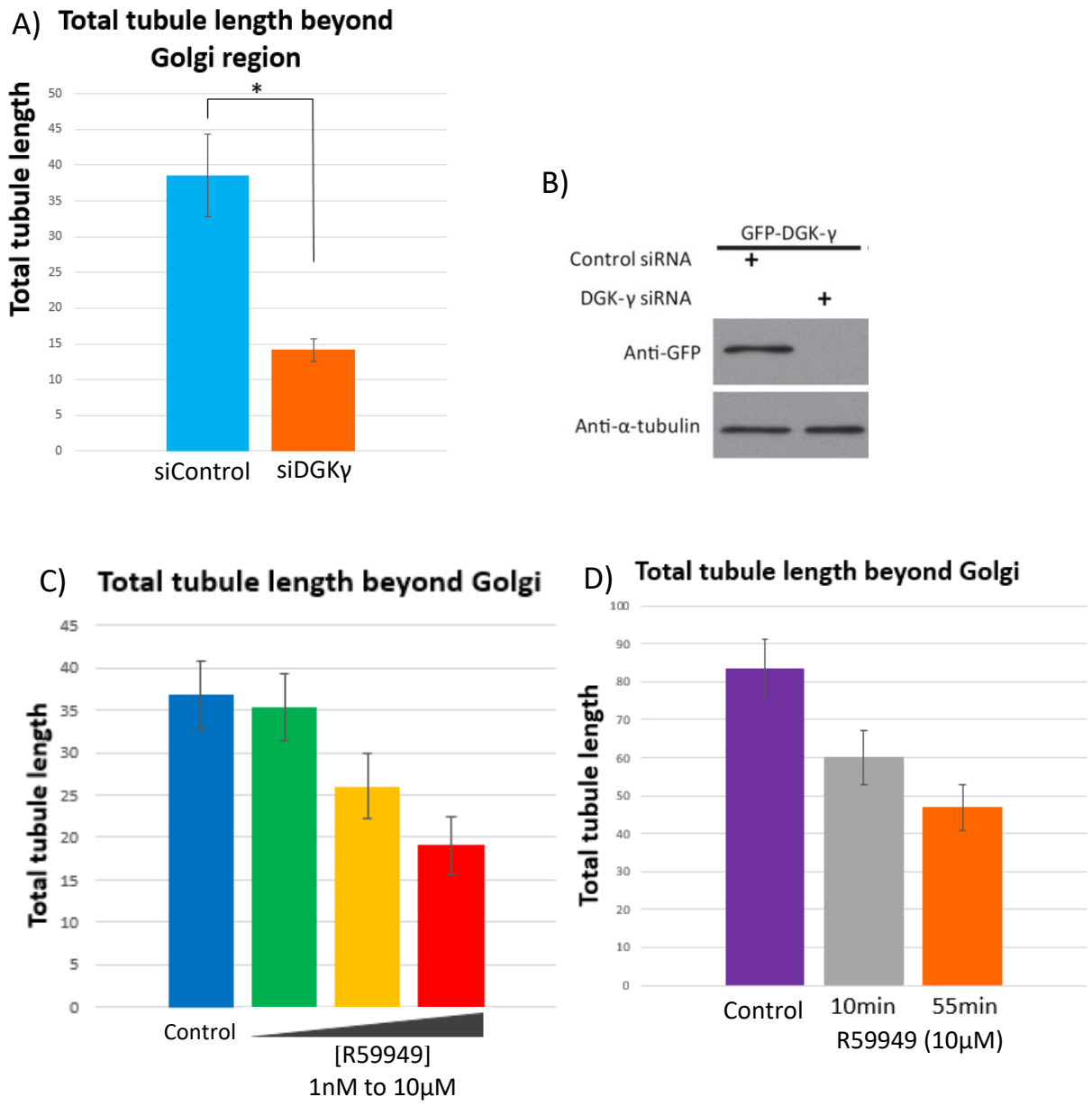

Figure 4. DGKγ involvement in formation of tubular cargo carriers at the Golgi.

Quantification of GP135-containing tubular cargo carriers at 45 minutes in a RUSH experiment in cells treated with A-B) siControl and siDGKγ RNA, with or without a rescue construct and C) a drug inhibitor of type I DGKs (R59949) at increasing dosages and D) varying exposure times. Experiments performed in HeLa cells: n=3, with each independent experiment measuring >100 cells for each condition.

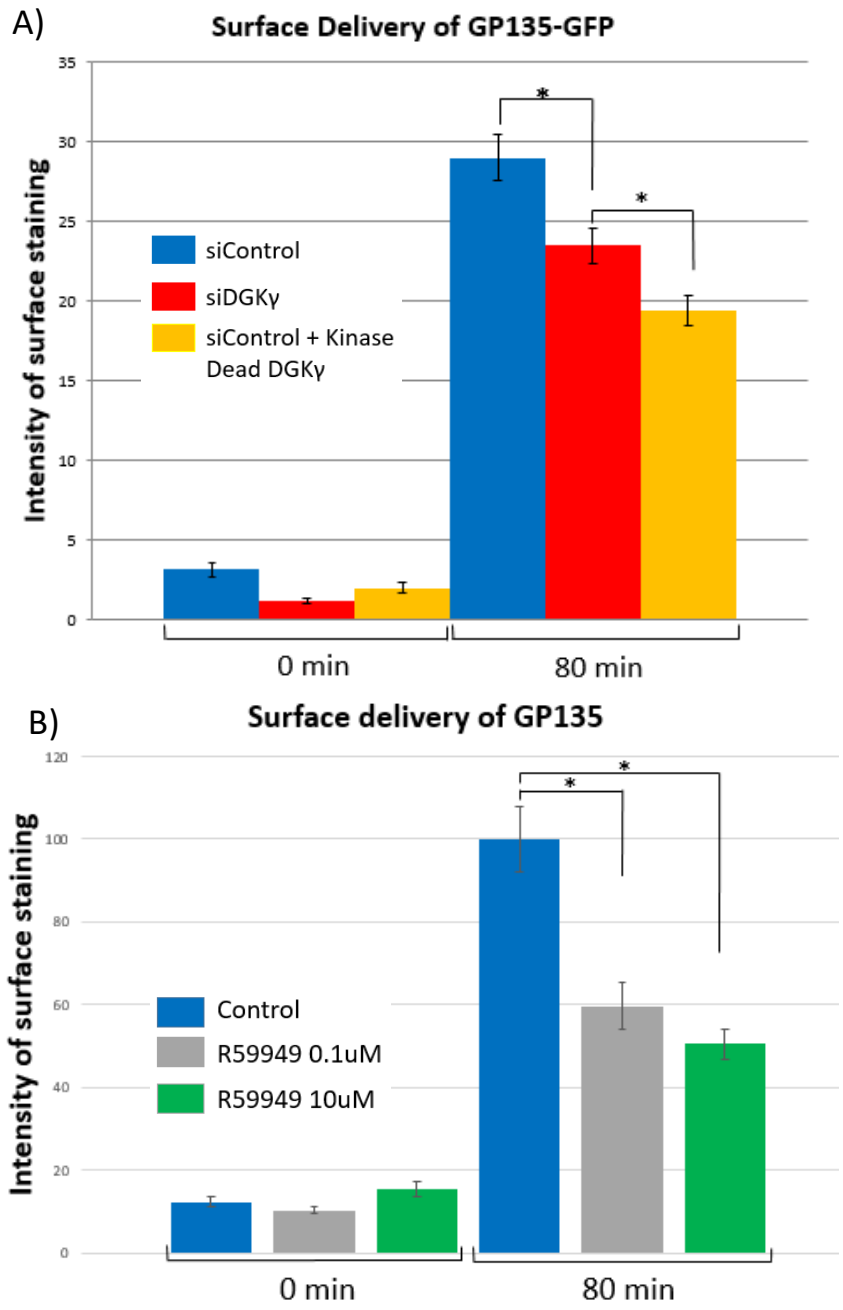

Figure 5. DGKγ involvement in trafficking of cargo to the PM. Delivery of GP135 from the ER to the PM at 0 min and 80min in a RUSH experiment in cells treated with A) siControl and siDGKγ RNA, with rescue constructs as indicated (WT= wild type, KD= kinase dead) and B) a drug inhibitor of type I DGKs (R59949) at increasing dosages. Experiments performed in HeLa cells: n=3, each experiment measuring >100 cells for each condition.

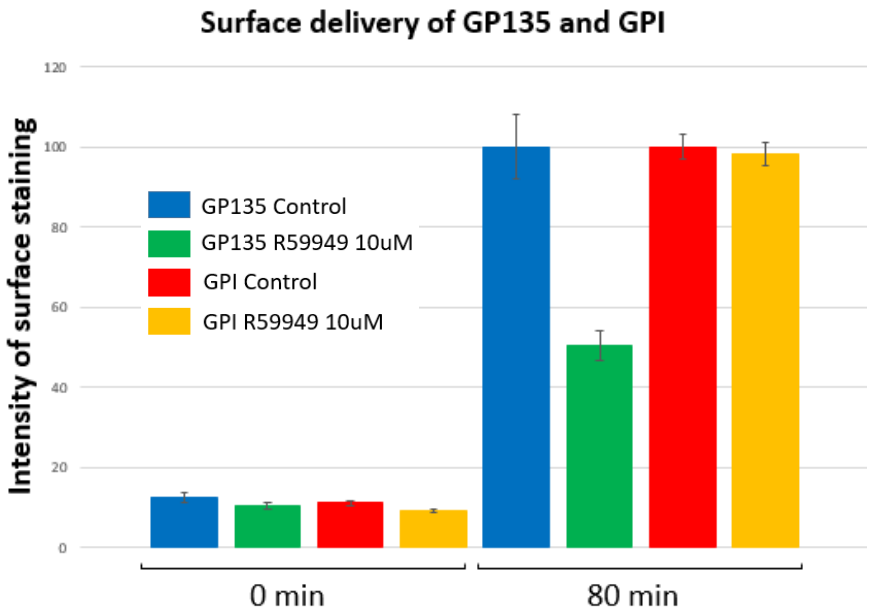

Figure 6. Cargo selectivity of DGKγ involvement in trafficking from the Golgi. Delivery of GP135 from the ER to the PM at 0 min and 80min in a RUSH experiment in cells treated with 10uM R59949 for 10min prior to trafficking assay. Experiments performed in HeLa cells: n=3, each experiment measuring >100 cells for each condition.

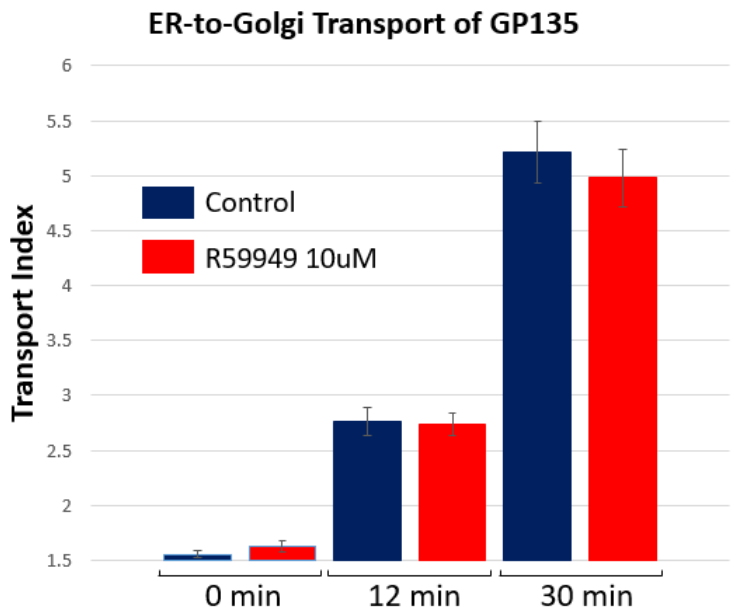

Figure 7. DGKγ involvement in trafficking from the ER. A) Delivery of GP135 from the ER to the Golgi at 0min, 15min, and 30min in a RUSH experiment in cells treated with 10uM R59949 for 10min prior to trafficking assay. Experiments performed in HeLa cells: n=1, experiment measuring >100 cells for each condition.

Figure 8. DGKγ involvement in Golgi structure homeostasis. A) Cells treated with 10uM R59949 for the indicated times, followed by a wash and the indicated recovery times, were stained with α-GPP130 antibody. The number of GPP130 positive particles was counted for each condition. B) Cells treated with siControl or siDGKγ were fixed and imaged with TEM. Images were blinded, and cells were scored for degree of cisternal stacking of Golgi membranes (0-4). Experiments performed in HeLa cells: A) n=4, each experiment measuring >200 cells; B) n=1, each condition having >30 cells.

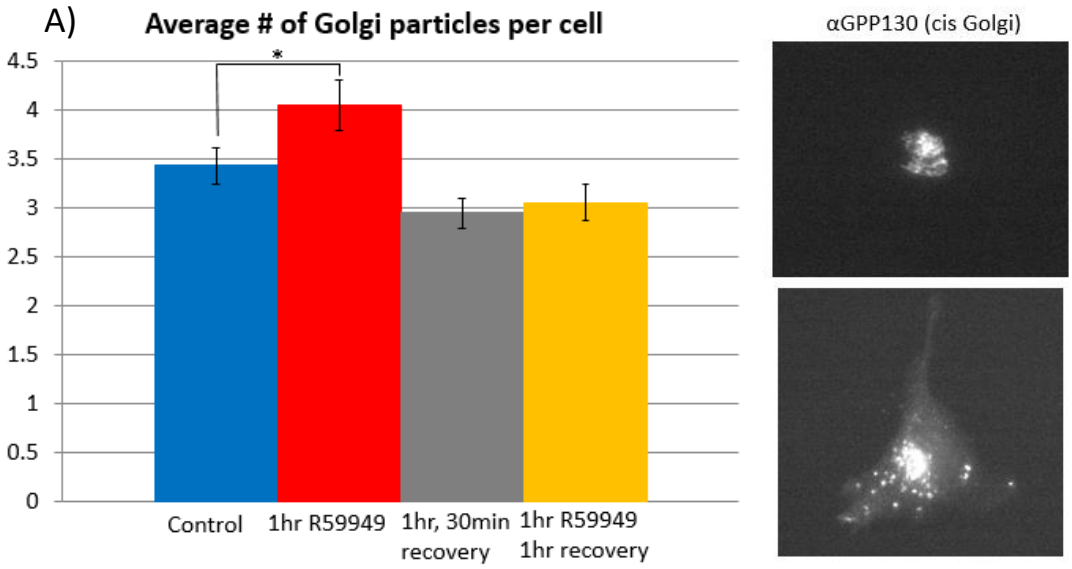
A)
Average # of Golgi particles per cell
4.5
4
3.5
3
2.5
2
1.5
1
0.5
0
*
Control
1hr R59949
1hr, 30min recovery
1hr R59949 1hr recovery
αGPP130 (cis Golgi)

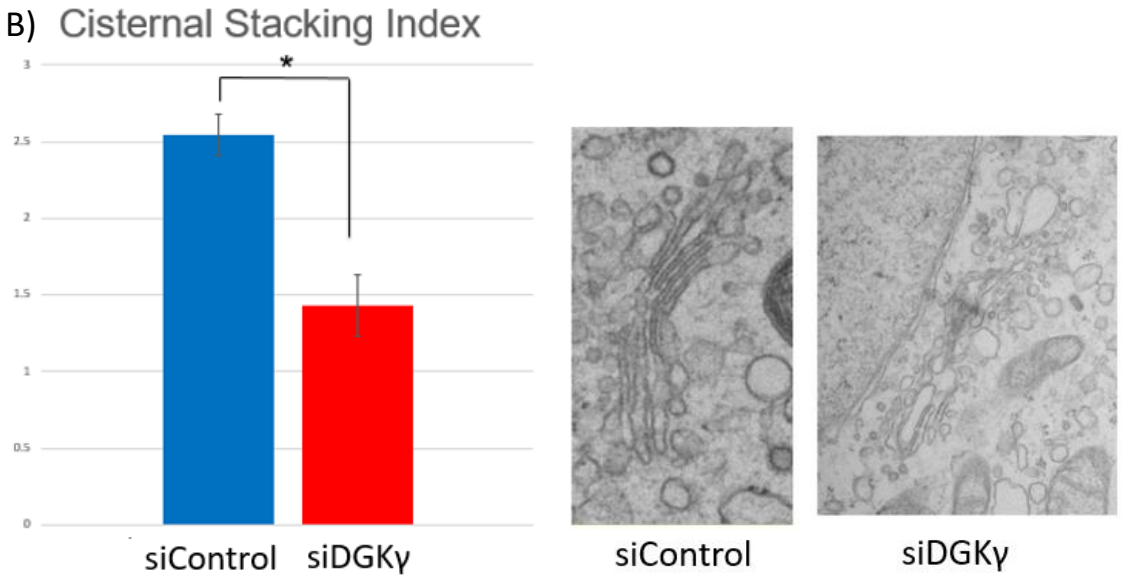
B) Cisternal Stacking Index
3
2.5
2
1.5
1
0.5
0
*
siControl
siDGKγ
siControl
siDGKγ

A)

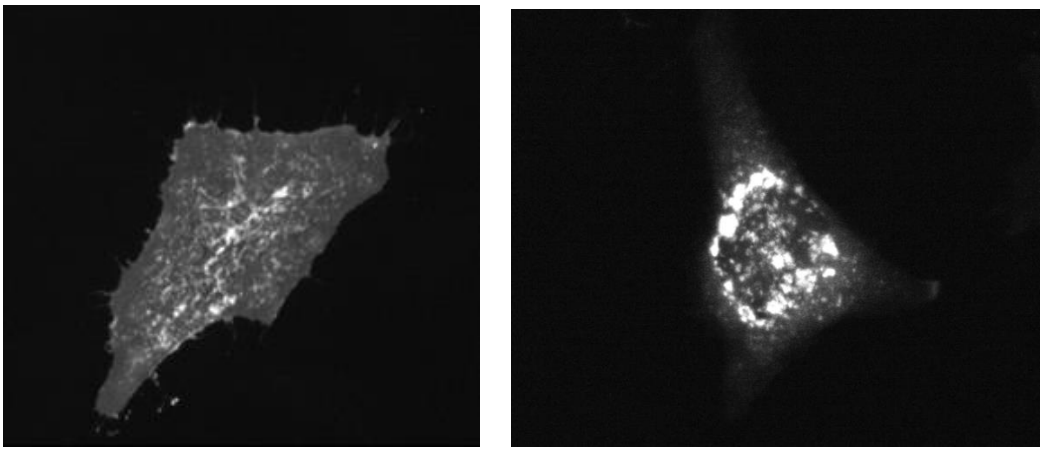

EGFP-DGKγ (predominant localization) EGFP-DGKγ (rare localization)

B)

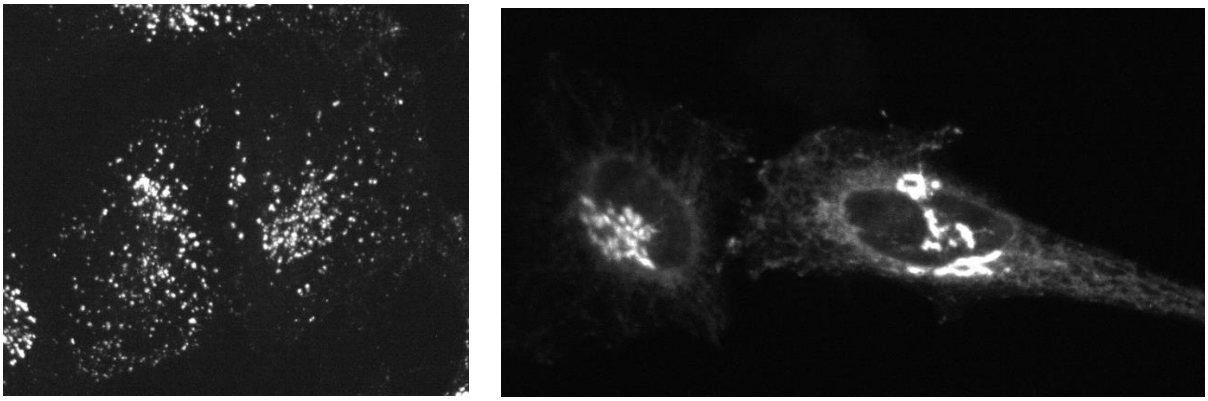

anti-DGKγ (predominant staining) anti-DGKγ (rare staining)

Figure 9. Localization of DGKγ. A) Localization of an EGFP-DGKγ construct in HeLa cells. B) Staining pattern of endogenous DGKγ in HeLa cells. Left panels for A) and B) show the predominant (>99%) localization, while right panels show rare but distinct localization.

Figure 10. Possible roles for DAG, PA and DGKγ in trafficking out of the TGN. PA (green lipid) and DAG (blue lipid) and their cellular targets of activation (indicated by green or blue text, respectively). DAG, PA, and DGKγ may operate in trafficking at the TGN through (1) signaling events, (2) tubule/vesicle budding, (3) tubule/vesicle fission, and (4) vesicle/tubule maturation. As DAG, PA and DGKγ may be positive or negative regulators of several events, and much remains unclear, all possibilities are considered here, regardless of how they relate to the data shown in this study. **(1) Signaling:** Numerous extracellular signals lead to phospholipase C (PLC) activation and production of DAG, which acts as a secondary signaling molecule activating numerous downstream pathways, some of which appear to regulate (next page)

trafficking out of the TGN. For instance, DAG activates PKCγ, which has been shown to regulate trafficking out of the ER and TGN. DAG may also modulate Trp and Orai1 channels, which have been shown to be involved in certain evoked exocytosis events, such as mast cell degranulation and neurotransmitter release. DGKγ may regulate these signaling pathways at the PM. **(2) Tubule budding:** DAG has been shown to be required for the initial budding of membrane tubules and vesicles at the TGN. It is thought that DAG's conical shape and ability to flip between bilayers may contribute to membrane reshaping. DAG may also play a role through its activation of PKC isoforms at the Golgi, which activate unknown downstream targets. In support of this, DGKγ has been shown to bind PKCγ and thus may deliver it to the TGN. DAG is also thought to recruit Arf-1, an important regulator of tubule formation, to the TGN. Finally, DAG may also activate Rho and Ras GTPases that remodel the actin cytoskeleton and may thus drive the extrusion of a tubule out of the TGN. PA may also play a role in budding, as it is a substrate for PLA_2. PLA_2 is required for membrane tubule formation, likely due to its production of LPA (indicated as a light grey lipid here), an inverse-conical lipid that produces positive

curvature in a membrane. Thus DGKγ here may feed PLA_2 its substrate to drive membrane budding, or it may act during budding (through PKCs) to progress the tubule down its life cycle. **(3) Tubule fission:** DAG activates PKCη and PKD, which is required for tubule fission. The downstream generation of PA at bud necks is thought to drive scission of the tubule. PA also activates PI(4)KIIIβ (required for fission) and dynamin, which may also drive fission at the TGN. **(4) Tubule maturation:** Here we show that DGKγ binds PPP6 and DENND4C. PPP6 acts in trafficking from the ER by dephosphorylating Sec31, allowing it to recycle for further rounds of vesicle formation. PPP6 may act in an analogous way at the TGN, through an unknown target. DENND4C acts as a GEF for Rab10, which is required for vesicle maturation and fusion with the PM. Thus DGKγ may act partly as a scaffold to position the machinery for tubule maturation at newly-formed tubules. DAG is important for activation of Rab3 and Munc13, which are involved in vesicle fusion with the PM; DGKγ here may be a negative regulator.

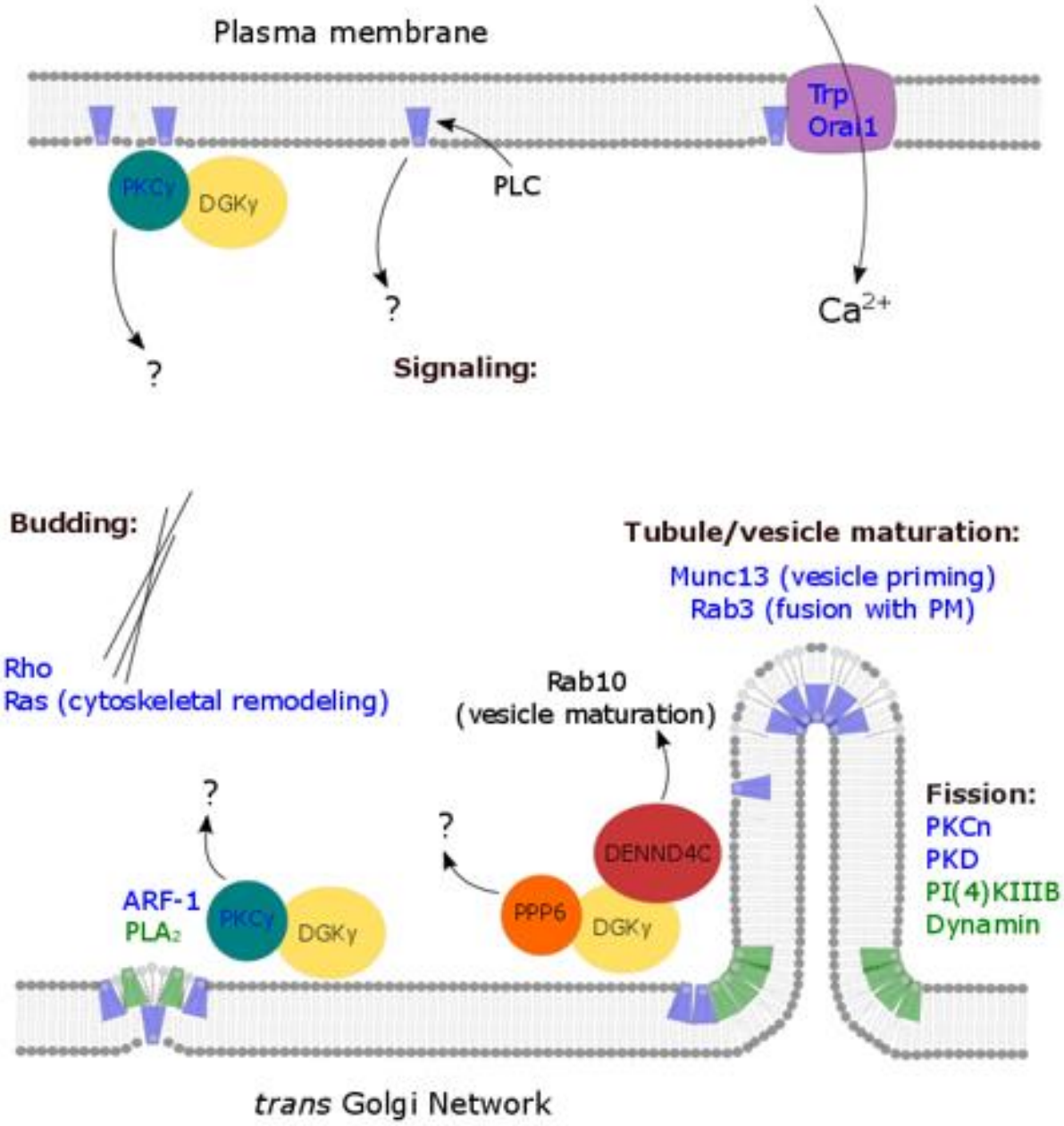
Plasma membrane
Trp
Orai1
PKCγ
DGKγ
PLC
?
Ca2+
?
Signaling:
Budding:
Rho
Ras (cytoskeletal remodeling)
Tubule/vesicle maturation:
Munc13 (vesicle priming)
Rab3 (fusion with PM)
Rab10
(vesicle maturation)
?
?
DENND4C
PPP6
DGKγ
ARF-1
PLA2
PKCγ
DGKγ
Fission:
PKCn
PKD
PI(4)KIIIB
Dynamin
trans Golgi Network

Table 1: Mammalian DGKs	Type-defining domains	Localization	Trafficking function
Type I (α, β γ)	EF-hand	α: PM[83], Golgi/TGN[33], MVB[84], endosome[21] β: PM[33] γ: PM[19, 33-38], nucleus[32], Golgi[39, 40]	α: + regulator TRE[21] β: - regulator CIE[20] γ: + regulator CIE[20], insulin secretion[25] and mast cell degranulation[37]
Type II (δ, η, κ)	Pleckstrin Homology (PH), Sterile Alpha Motif (SAM)	δ: PM[85], ER[26] η, κ: ER[26]	δ: + reg. CIE/ -reg CME[17, 20], - reg COPII function[26] η, κ: none
Type III (ε)	Transmembrane domain	PM?	none
Type IV (ζ, ι)	Nuclear localization signal, PKZ domain	ι: Nuclear[86], PM[22] ζ: Nuclear[86], PM[33], endosome[79]	ι: + regulator glutamate release[22] ζ: - reg transferrin recycling[79], + reg phagocytosis[87, 88]
Type V (θ)	Pleckstrin Homology (PH), Ras-association domain	PM[23]	- regulator acetylcholine release[23], synaptic vesicle recycling[24]
Abbreviations: TRE: tubular recycling endosome; CME: clathrin-mediated endocytosis; CIE: clathrin-independent endocytosis; reg: regulator			

Table 1. Mammalian diacylglycerol kinases (DGK) in membrane trafficking.

protein	count	count_h	count_l	gmean	log_gm	orf	description
APLP2	5	5	0	0.00288	-8.44136	APLP2	amyloid beta (A4) precursor-like protein 2
DGKA,DGKG	7	7	0	0.00801	-6.96428	DGKA	diacylglycerol kinase, alpha 80kDa
DGKG	1030	947	83	0.01333	-6.22958	DGKG	diacylglycerol kinase, gamma 90kDa
PPP6R3	71	68	3	0.02899	-5.1082	PPP6R3	protein phosphatase 6, regulatory subunit 3
PPP6C	35	30	5	0.04099	-4.6086	PPP6C	protein phosphatase 6, catalytic subunit
RNF219	6	6	0	0.05777	-4.11362	RNF219	ring finger protein 219
RHOT1	6	6	0	0.06267	-3.99597	RHOT1	ras homolog gene family, member T1
FAM115A	8	7	1	0.10081	-3.31024	FAM115A	family with sequence similarity 115, member A
DGKA,DGKB,DGKG	8	8	0	0.10347	-3.27266	DGKA	diacylglycerol kinase, alpha 80kDa
MID1	5	5	0	0.10415	-3.2633	MID1	midline 1 (Opitz/BBB syndrome)
PPP2R2A	16	14	2	0.11598	-3.10807	PPP2R2A	protein phosphatase 2, regulatory subunit B, alp
TUBB2B,TUBB2A	8	7	1	0.11676	-3.09835	TUBB2B	tubulin, beta 2B class IIb
PDLIM7	9	8	1	0.12334	-3.01931	PDLIM7	PDZ and LIM domain 7 (enigma)
CPS1	9	9	0	0.12629	-2.98517	CPS1	carbamoyl-phosphate synthase 1, mitochondrial
SKIV2L	12	10	2	0.12844	-2.96087	SKIV2L	superkiller viralicidic activity 2-like (S. cerevisiae
NUBP2	9	9	0	0.13501	-2.88882	NUBP2	nucleotide binding protein 2
MAD2L1	9	7	2	0.137	-2.86771	MAD2L1	MAD2 mitotic arrest deficient-like 1 (yeast)
PPP2CA,PPP2CB,PPP4	5	4	1	0.13833	-2.85386	PPP2CA	protein phosphatase 2, catalytic subunit, alpha
TMX3	7	7	0	0.13958	-2.84081	TMX3	thioredoxin-related transmembrane protein 3
PPP2R2A,PPP2R2D	5	5	0	0.14705	-2.76558	PPP2R2A	protein phosphatase 2, regulatory subunit B, alp
ACOT8	5	5	0	0.15147	-2.72286	ACOT8	acyl-CoA thioesterase 8
USP15	29	26	3	0.15188	-2.71897	USP15	ubiquitin specific peptidase 15
ANKRD28	20	20	0	0.15884	-2.65434	ANKRD28	ankyrin repeat domain 28
GPX1	7	5	2	0.16408	-2.60749	GPX1	glutathione peroxidase 1
ZNF24	16	15	1	0.16558	-2.59443	ZNF24	zinc finger protein 24
GNB1L	5	3	2	0.17409	-2.52207	GNB1L	guanine nucleotide binding protein (G protein),
VPS4B	5	4	1	0.17669	-2.50071	VPS4B	vacuolar protein sorting 4 homolog B (S. cerevisi

Table 2. DGKγ-interacting proteins. SILAC-MS results for EGFP-DGKγ expressed in HeLa cells. Control EGFP was analyzed in parallel to eliminate EGFP-interacting peptides. Peptides of particular interest are highlighted in yellow.

protein	count	count_h	count_l	gmean	log_gm	orf	description
DGKG	471	439	32	0.0342	-4.86982	DGKG	diacylglycerol kinase, gamma
PPP6C	49	45	4	0.04404	-4.50519	PPP6C	protein phosphatase 6, cataly
PPP6R3	79	78	1	0.06014	-4.05546	PPP6R3	protein phosphatase 6, regul
PPP6R2	11	11	0	0.07888	-3.66418	PPP6R2	protein phosphatase 6, regul
TUBB4	10	10	0	0.10862	-3.2026	TUBB4	
ANKRD28	38	38	0	0.11675	-3.09849	ANKRD28	ankyrin repeat domain 28
WDR77	47	42	5	0.11984	-3.06084	WDR77	WD repeat domain 77
SETD2	10	10	0	0.12242	-3.03012	SETD2	SET domain containing 2
RCN2	40	35	5	0.13695	-2.86826	RCN2	reticulocalbin 2, EF-hand calc
PRMT5	76	70	6	0.15092	-2.72811	PRMT5	protein arginine methyltransf
TTC37	32	32	0	0.16515	-2.59819	TTC37	tetratricopeptide repeat dom
PPP2R2A	16	15	1	0.1673	-2.57952	PPP2R2A	protein phosphatase 2, regul
AKAP8L	26	24	2	0.16792	-2.57413	AKAP8L	A kinase (PRKA) anchor protei
BCR	15	15	0	0.16922	-2.563	BCR	breakpoint cluster region
DENND4C	10	10	0	0.16925	-2.56277	DENND4C	DENN/MADD domain containi
PPP2CA,PP	37	29	8	0.16952	-2.56046	PPP2CA	protein phosphatase 2, cataly
SKIV2L	12	12	0	0.17275	-2.53323	SKIV2L	superkiller viralicidic activity
MAGED1	13	13	0	0.17584	-2.50768	MAGED1	melanoma antigen family D,
ZMYM2	16	16	0	0.18384	-2.44346	ZMYM2	zinc finger, MYM-type 2
RNF219	17	17	0	0.19223	-2.37913	RNF219	ring finger protein 219
TUBB6,TU	10	8	2	0.19558	-2.35417	TUBB6	tubulin, beta 6 class V
USP9Y,USI	**34**	**34**	**0**	**0.20113**	**-2.31383**	**USP9Y**	**ubiquitin specific peptidase 9, Y-**
RANBP9	12	11	1	0.20233	-2.30523	RANBP9	RAN binding protein 9
TUBB6,TU	10	7	3	0.20373	-2.29526	TUBB6	tubulin, beta 6 class V
SEC13	14	13	1	0.2057	-2.28137	SEC13	SEC13 homolog (S. cerevisiae)
USP15	21	20	1	0.20764	-2.26786	USP15	ubiquitin specific peptidase
TUBB6,TU	22	16	6	0.2115	-2.24127	TUBB6	tubulin, beta 6 class V

Table 3. DGKγCA-interacting proteins. SILAC-MS results for a constitutively active EGFP-DGKγ (Δ1-259) construct expressed in HeLa cells. Control EGFP was analyzed in parallel to eliminate EGFP-interacting peptides. Peptides of particular interest are highlighted in yellow.

CHAPTER FIVE

EXPERIMENTAL PROCEDURES

Cell culture and transfection

HeLa cells were maintained in modified Eagle's minimal essential medium (MEM, Invitrogen 61100-087) with 10% fetal bovine serum (FBS, Life Technologies, CA) at 37ºC, 5% CO_2, and 95% humidity. For transfections in 35 mm dishes, 1µg of DNA and/or siRNA (final concentration on cells = 30 nM) was incubated with 2 µL of Lipofectamine 2000 (Thermofisher 11668-019) for 20 min at room temperature. This was then added dropwise into 1 mL of MEM (no serum) in a dish of cells grown to 80% confluency. Cells were incubated with the transfection complex for 5-6 h, after which the MEM was replaced with complete media. All experiments were performed 24 h or 48 h (as indicated) after the addition of the transfection complex.

RUSH experiments

RUSH experiments were performed as previously described[28]. Briefly, cells grown in 35 mm dishes were transfected with RUSH plasmids for 24 h, then washed 3x's with MEM (no serum) and allowed to recover in 1.5 mL of MEM (no serum) at 37ºC for 10 min. 4 mM biotin was added to a final concentration of 40 nM, beginning the timecourse. At the indicated timepoints, coverslips were removed from the MEM + biotin and fixed in 3.7% Formalin in 1x PBS for 10 min. Coverslips were mounted on 8 µL of ProLong Antifade Mountant (Life Technologies P36970) and allowed to cure overnight.

Plasmids, siRNA and reagents

siRNA targeting human DGKγ was purchased from GenePharma Co., Ltd. (Shanghai, China) using sequence 5' – GGGUGGGAGCCUCAAACAAtt – 3'. A plasmid for DGKγ was purchased from Harvard PlasmID (HsCD00026096) and edited to match the sequence for human isoform 1 (NM_001346.2, with the following naturally-occurring mutations: T142S, R316K). This construct was cloned into pEGFP-C3 and mCherry-C2 vectors using XhoI and HindIII restriction sites. siRNA-resistant constructs of the above were generated using QuickChange II (Agilent Technologies) using two silent mutations within the target siRNA sequence. A kinase dead construct was generated by mutating G494D[18], again using QuickChange II. A constitutively active construct was made by amplifying the Δ1-259 portion of DGKγ and cloning this into pEGFP-C3 using HindIII and XhoI restriction sites. Bi-cistronic RUSH plasmids (Str-KDEL_SBP-GFP-GP135 and Str-KDEL_SBP-GFP-GPI) were kind gifts of Frank Perez. Type II DGK inhibitor R59949 was purchased from Santa Cruz (SCBT-sc-3551).

Electron Microscopy

HeLa cells grown to ~90% confluency were fixed (0.83% glutaraldehyde, 0.67% OsO_4 in 0.1 M Na Cacodylate, pH 7.4) for 1 h on ice, washed 3x's with cold 0.1 M Na Cacodylate, pH 7.4, stained with 0.25% uranyl acetate (in H_20) for 15-30 min, washed 3x with cold 0.1 M Na Cacodylate, pH 7.4, dehydrated with Pharmco-Aaper 200-proof EtOH (washed 3x each with 50%, 70%, 95%, 100% solutions), etched with 100% propylene oxide, scraped off the dishes, and embedded in Epon resin (48 h polymerization). Embedded cells were then sectioned and stained with 3.5 mg/mL Pb Acetate solution (5 min) and 40 mg/mL Uranyl Acetate solution (20 min) and imaged on a FEI Philips Morgagni 268 transmission electron microscope at about 80 kV using Morigami Software.

SILAC Mass Spectroscopy

HEK293T cells were grown a minimum of five generations in DMEM with 10% dialyzed FBS (Sigma) containing either light (L-Lysine-$^{13}C_6$,$^{15}N_2$ hydrochloride, Sigma #608041) or heavy (L-Arginine-$^{13}C_6$,$^{15}N_4$ hydrochloride, Sigma #608033) amino acids. Cells grown in heavy media were transfected in two 15 cm dishes with EGFP-DGKγ wild type or constitutively-active constructs, while cells grown in light media were transfected with pEGFP. After 48 h, cells were lysed in RIPA buffer (No SDS, 50 mM NaF, 50 mM Tris-Cl pH 7.5, 150 mM NaCl, 1% NP-40, 5 mM EDTA, 0.25% sodium deoxycholate with protease inhibitors (Roche). The lysates were incubated with GFP-Trap beads (ChromoTek) overnight at 4^{o}C. Transfection and immunoprecipitation of EGFP and EGFP-DGKγ were confirmed by SDS-PAGE and Western blot analysis probing for GFP. Samples were boiled 5 min, incubated with DTT (final 10 mM) for 15 min to reduce, and alkylated with iodoacetamide (final concentration 28 mM). Heavy and light samples were mixed and proteins were precipitated on ice for 30 min with a 50% acetone, 49.9% ethanol, 0.1% acetic acid solution, washed once in the same buffer, suspended in 8 M urea/50 mM Tris pH 8.0, and diluted with three volumes of 50 mM Tris pH 8.0, 150 mM NaCl. Proteins were digested overnight on a nutator at 37°C with 1μg Gold trypsin (Promega). Samples were then acidified with 10% trifluoroacetic acid (TFA) and 10% formic acid using a glass syringe and washed on pre-conditioned C18 column (WAT0549-55) with 0.1% HAc. Samples were eluted with 80% acetonitrile (ACN), 0.1% acetic acid into silanized vials (National Scientific) and evaporated using a SpeedVac. Samples were suspended in H2O with ~1% formic acid and 70% ACN. Peptides were then separated using hydrophilic interaction liquid chromatography (HILIC) on an Ultimate 300 LC (Dionex). Samples were evaporated with a SpeedVac and re-suspended in 0.1% TFA with 0.1 pM angiotensin internal standard. Samples

were injected into a Thermo LTQ Orbitrap XL mass spectrometer and the data were processed with the SORCERER platform.

Fluorescence microscopy

HeLa cells grown on glass coverslips were fixed in 3.7% paraformaldehyde for 15 min, washed 3 times with PBS, and permeabilized with 0.05% saponin in PBS or 0.1% Triton in PBS for 20 min. Coverslips were stained with primary antibodies diluted in 0.05% saponin in PBS for 1 h at 4°C. Coverslips were washed 3 times with 0.05% saponin in PBS, and stained with secondary antibodies diluted in 0.05 % in PBS for 45 min at room temperature. Mouse anti-SBP antibody (Santa Cruz sc-101595) was used at 1:1,000. Rabbit anti-GPP130 (Covance PRB-144C) was used at 1:600. Goat anti-mouse Cy5 (Jackson ImmunoResearch 115-175-146) was used at 1:200. Goat anti-rabbit FITC (Jackson ImmunoResearch 111-485-045) was used at 1:400. Coverslips were washed 3 times with 0.05% saponin in PBS and mounted on 8 uL of ProLong Antifade Mountant (Life Technologies P36970) and allowed to cure overnight. Wide-field epifluorescence imaging was conducted on an Axioscope II (Carl Zeiss, Inc.) with Plan-Apo 40x/NA1.4 air objective with an Orca II camera (Hamamatsu Photonics) using Openlab software (PerkinElmer). Golgi membrane tubules were imaged on a spinning-disk confocal microscope: an Eclipse TE2000-U (Nikon) with Plan-Apo 60x/NA1.4 oil objective with an Ultraview LCI (PerkinElmer), a 1394 ORCA-ER camera (Hamamatsu Photonics) and Ultraview imaging software (PerkinElmer).

Cell lysates, antibodies, and immunoblotting

Cells were washed 3 times with ice-cold PBS and lysed by incubation in sample buffer (125 mM Tris pH 6.8, 4% SDS, 20% glycerol, 10% 2-mercaptoethanol, 50 µg/mL bromophenol blue) for 10 min, followed by scraping. Lysates were analyzed by SDS-PAGE (10% gel, run at 120 V for

80 min), transferred onto nitrocellulose membranes (Whatman Inc., United Kingdom) (transferred at 15 mA for 80 min). Rabbit antibodies against GFP were diluted 1:1000 and were a gift from Dr. A. Bretscher (Cornell University). HRP-conjugated secondary antibodies against rabbit and mouse were diluted 1:20,000 (Jackson ImmunoResearch, PA).

Statistical analysis

All bar graphs represent mean ± SEM. Student's t tests were performed: values <0.05 were considered statistically significant.

REFERENCES

1. Ziolkowska NE, Christiano R, Walther TC. Organized living: formation mechanisms and functions of plasma membrane domains in yeast. Trends Cell Biol. 2012;22(3):151-8.

2. Faini M, Beck R, Wieland FT, Briggs JA. Vesicle coats: structure, function, and general principles of assembly. Trends Cell Biol. 2013;23(6):279-88.

3. Hirst J, Borner GH, Antrobus R, Peden AA, Hodson NA, Sahlender DA, et al. Distinct and overlapping roles for AP-1 and GGAs revealed by the "knocksideways" system. Curr Biol. 2012;22(18):1711-6.

4. Robinson MS. Adaptable adaptors for coated vesicles. Trends Cell Biol. 2004;14(4):167-74.

5. Wakana Y, van Galen J, Meissner F, Scarpa M, Polishchuk RS, Mann M, et al. A new class of carriers that transport selective cargo from the trans Golgi network to the cell surface. EMBO J. 2012;31(20):3976-90.

6. Sciaky N, Presley, J., Smith, C., Zaal, K., Cole, N., Moreira, J., Terasaki, M., Siggia, E., Lippincott-Schwartz, J. Golgi tubule traffic and the effects of brefeldin A visualized in living cells. J Cell Biol. 1997;139(5):1137-55.

7. Fernandez-Ulibarri I, Vilella M, Lazaro-Dieguez F, Sarri E, Martinez SE, Jimenez N, et al. Diacylglycerol is required for the formation of COPI vesicles in the Golgi-to-ER transport pathway. Mol Biol Cell. 2007;18(9):3250-63.

8. Maeda Y, Beznoussenko GV, Van Lint J, Mironov AA, Malhotra V. Recruitment of protein kinase D to the trans-Golgi network via the first cysteine-rich domain. EMBO J. 2001;20(21):5982-90.

9. Asp L, Kartberg F, Fernandez-Rodriguez J, Smedh M, Elsner M, Laporte F, et al. Early stages of Golgi vesicle and tubule formation require diacylglycerol. Mol Biol Cell. 2009;20(3):780-90.

10. McMaster CR. Lipid metabolism and vesicle trafficking: more than just greasing the transport machinery. Biochemistry and cell biology = Biochimie et biologie cellulaire. 2001;79(6):681-92.

11. Huijbregts RP, Topalof L, Bankaitis VA. Lipid metabolism and regulation of membrane trafficking. Traffic. 2000;1(3):195-202.

12. Roth MG. Lipid regulators of membrane traffic through the Golgi complex. Trends Cell Biol. 1999;9(5):174-9.

13. Siddhanta A, Shields D. Secretory vesicle budding from the trans-Golgi network is mediated by phosphatidic acid levels. J Biol Chem. 1998;273(29):17995-8.

14. Gomez-Merino FC, Brearley CA, Ornatowska M, Abdel-Haliem ME, Zanor MI, Mueller-Roeber B. AtDGK2, a novel diacylglycerol kinase from Arabidopsis thaliana, phosphorylates 1-stearoyl-2-arachidonoyl-sn-glycerol and 1,2-dioleoyl-sn-glycerol and exhibits cold-inducible gene expression. J Biol Chem. 2004;279(9):8230-41.

15. Topham MK, Prescott SM. Mammalian diacylglycerol kinases, a family of lipid kinases with signaling functions. J Biol Chem. 1999;274(17):11447-50.

16. Badola P, Sanders CR, 2nd. Escherichia coli diacylglycerol kinase is an evolutionarily optimized membrane enzyme and catalyzes direct phosphoryl transfer. J Biol Chem. 1997;272(39):24176-82.

17. Miner GE, Starr ML, Hurst LR, Fratti RA. Characterization of the yeast DGK1-encoded CTP-dependent diacylglycerol kinase. Traffic. 2017;18(5):315-329.

18. van Blitterswijk W, Houssa, B. Properties and functions of diacylglycerol kinase. Cellular signalling. 2000;12:595-605.

19. Yamada K, Sakane F, Imai S-i, Tsushima S, Murakami T, Kanoh H. Regulatory role of diacylglycerol kinase γ in macrophage differentiation of leukemia cells. Biochemical and Biophysical Research Communications. 2003;305(1):101-7.

20. Pelkmans L, Fava E, Grabner H, Hannus M, Habermann B, Krausz E, et al. Genome-wide analysis of human kinases in clathrin- and caveolae/raft-mediated endocytosis. Nature. 2005;436(7047):78-86.

21. Xie S, Naslavsky N, Caplan S. Diacylglycerol kinase alpha regulates tubular recycling endosome biogenesis and major histocompatibility complex class I recycling. J Biol Chem. 2014;289(46):31914-26.

22. Yang J, Seo J, Nair R, Han S, Jang S, Kim K, et al. DGKiota regulates presynaptic release during mGluR-dependent LTD. EMBO J. 2011;30(1):165-80.

23. Miller KG, Emerson MD, Rand JB. Goalpha and diacylglycerol kinase negatively regulate the Gqalpha pathway in C. elegans. Neuron. 1999;24(2):323-33.

24. Goldschmidt HL, Tu-Sekine B, Volk L, Anggono V, Huganir RL, Raben DM. DGKtheta Catalytic Activity Is Required for Efficient Recycling of Presynaptic Vesicles at Excitatory Synapses. Cell Rep. 2016;14(2):200-7.

25. Kurohane Kaneko Y, Kobayashi Y, Motoki K, Nakata K, Miyagawa S, Yamamoto M, et al. Depression of type I diacylglycerol kinases in pancreatic beta-cells from male mice results in impaired insulin secretion. Endocrinology. 2013;154(11):4089-98.

26. Nagaya H, Wada I, Jia YJ, Kanoh H. Diacylglycerol kinase delta suppresses ER-to-Golgi traffic via its SAM and PH domains. Mol Biol Cell. 2002;13(1):302-16.

27. Martinez-Alonso E, Tomas M, Martinez-Menarguez JA. Golgi tubules: their structure, formation and role in intra-Golgi transport. Histochem Cell Biol. 2013;140(3):327-39.

28. Boncompain G, Perez F. Synchronizing protein transport in the secretory pathway. Curr Protoc Cell Biol. 2012;Chapter 15:Unit 15 9.

29. Chen Y, Gershlick DC, Park SY, Bonifacino JS. Segregation in the Golgi complex precedes export of endolysosomal proteins in distinct transport carriers. J Cell Biol. 2017;Epub ahead of print.

30. Mukherjee S, Zeitouni S, Cavarsan CF, Shapiro LA. Increased seizure susceptibility in mice 30 days after fluid percussion injury. Frontiers in neurology. 2013;4:28.

31. Lane JD, Lucocq J, Pryde J, Barr FA, Woodman PG, Allan VJ, et al. Caspase-mediated cleavage of the stacking protein GRASP65 is required for Golgi fragmentation during apoptosis. J Cell Biol. 2002;156(3):495-509.

32. Matsubara T, Shirai Y, Miyasaka K, Murakami T, Yamaguchi Y, Ueyama T, et al. Nuclear transportation of diacylglycerol kinase gamma and its possible function in the nucleus. J Biol Chem. 2006;281(10):6152-64.

33. Shirai Y, Segawa S, Kuriyama M, Goto K, Sakai N, Saito N. Subtype-specific translocation of diacylglycerol kinase alpha and gamma and its correlation with protein kinase C. J Biol Chem. 2000;275(32):24760-6.

34. Tsushima S, Kai M, Yamada K, Imai S, Houkin K, Kanoh H, et al. Diacylglycerol kinase gamma serves as an upstream suppressor of Rac1 and lamellipodium formation. J Biol Chem. 2004;279(27):28603-13.

35. Yamaguchi Y, Shirai Y, Matsubara T, Sanse K, Kuriyama M, Oshiro N, et al. Phosphorylation and up-regulation of diacylglycerol kinase gamma via its interaction with protein kinase C gamma. J Biol Chem. 2006;281(42):31627-37.

36. Yasuda S, Kai M, Imai S, Kanoh H, Sakane F. Diacylglycerol kinase gamma interacts with and activates beta2-chimaerin, a Rac-specific GAP, in response to epidermal growth factor. FEBS Lett. 2007;581(3):551-7.

37. Sakuma M, Shirai Y, Ueyama T, Saito N. Diacylglycerol kinase gamma regulates antigen-induced mast cell degranulation by mediating Ca(2+) influxes. Biochem Biophys Res Commun. 2014;445(2):340-5.

38. Kaneko YK, Ishikawa T. Diacylglycerol Signaling Pathway in Pancreatic β-Cells: An Essential Role of Diacylglycerol Kinase in the Regulation of Insulin Secretion. Biol Pharm Bull. 2015;38(5):669-73.

39. Kobayashi N, Hozumi Y, Ito T, Hosoya T, Kondo H, Goto K. Differential subcellular targeting and activity-dependent subcellular localization of diacylglycerol kinase isozymes in transfected cells. Eur J Cell Biol. 2007;86(8):433-44.

40. Nakano T, Hozumi Y, Goto K, Wakabayashi I. Involvement of diacylglycerol kinase gamma in modulation of iNOS synthesis in Golgi apparatus of vascular endothelial cells. Naunyn Schmiedebergs Arch Pharmacol. 2012;385(8):787-95.

41. Yanagisawa K, Yasuda S, Kai M, Imai S, Yamada K, Yamashita T, et al. Diacylglycerol kinase alpha suppresses tumor necrosis factor-alpha-induced apoptosis of human melanoma cells through NF-kappaB activation. Biochim Biophys Acta. 2007;1771(4):462-74.

42. Shirai Y. Analysis of molecular mechanism regulating spatio-temporal localization and activity of protein kinase C and diacylglycerol kinase using live imaging. Nihon Yakurigaku Zasshi. 2004;123(3):186-96.

43. Buccione R, Bannykh S, Santone I, Baldassarre M, Facchiano F, Bozzi Y, et al. Regulation of Constitutive Exocytic Transport by Membrane Receptors. Journal of Biological Chemistry. 1996;271(7):3523-33.

44. Bhandari D, Zhang J, Menon S, Lord C, Chen S, Helm JR, et al. Sit4p/PP6 regulates ER-to-Golgi traffic by controlling the dephosphorylation of COPII coat subunits. Mol Biol Cell. 2013;24(17):2727-38.

45. Yoshimura S, Gerondopoulos A, Linford A, Rigden DJ, Barr FA. Family-wide characterization of the DENN domain Rab GDP-GTP exchange factors. J Cell Biol. 2010;191(2):367-81.

46. Bechler ME, Doody AM, Racoosin E, Lin L, Lee KH, Brown WJ. The phospholipase complex PAFAH Ib regulates the functional organization of the Golgi complex. J Cell Biol. 2010;190(1):45-53.

47. Schmidt JA, Kalkofen DN, Donovan KW, Brown WJ. A role for phospholipase A2 activity in membrane tubule formation and TGN trafficking. Traffic. 2010;11(12):1530-6.

48. Ha KD, Clarke BA, Brown WJ. Regulation of the Golgi complex by phospholipid remodeling enzymes. Biochim Biophys Acta. 2012;1821(8):1078-88.

49. Schmidt JA, Brown WJ. Lysophosphatidic acid acyltransferase 3 regulates Golgi complex structure and function. J Cell Biol. 2009;186(2):211-8.

50. Valente C, Turacchio G, Mariggio S, Pagliuso A, Gaibisso R, Di Tullio G, et al. A 14-3-3gamma dimer-based scaffold bridges CtBP1-S/BARS to PI(4)KIIIbeta to regulate post-Golgi carrier formation. Nat Cell Biol. 2012;14(4):343-54.

51. McMahon HT, Boucrot E. Membrane curvature at a glance. J Cell Sci. 2015;128(6):1065-70.

52. Ron D, Kazanietz MG. New insights into the regulation of protein kinase C and novel phorbol ester receptors. FASEB J. 1999;13(13):1658-76.

53. Brose N, Rosenmund C. Move over protein kinase C, you've got company- alternative cellular effectors of diacylglycerol and phorbol esters. J Cell Sci. 2002;115(Pt 23):4399-411.

54. Bard F, Malhotra V. The formation of TGN-to-plasma-membrane transport carriers. Annu Rev Cell Dev Biol. 2006;22:439-55.

55. Diaz Anel AM, Malhotra V. PKCeta is required for beta1gamma2/beta3gamma2- and PKD-mediated transport to the cell surface and the organization of the Golgi apparatus. J Cell Biol. 2005;169(1):83-91.

56. Simon JP, Ivanov IE, Adesnik M, Sabatini DD. The production of post-Golgi vesicles requires a protein kinase C-like molecule, but not its phosphorylating activity. J Cell Biol. 1996;135(2):355-70.

57. Fang Y, Vilella-Bach M, Bachmann R, Flanigan A, Chen J. Phosphatidic acid-mediated mitogenic activation of mTOR signaling. Science (New York, NY). 2001;294(5548):1942-5.

58. Tesfai Y, Brereton HM, Barritt GJ. A diacylglycerol-activated Ca2+ channel in PC12 cells (an adrenal chromaffin cell line) correlates with expression of the TRP-6 (transient receptor potential) protein. The Biochemical journal. 2001;358(Pt 3):717-26.

59. Huang CC, Yang DM, Lin CC, Kao LS. Involvement of Rab3A in vesicle priming during exocytosis: interaction with Munc13-1 and Munc18-1. Traffic. 2011;12(10):1356-70.

60. Hofmann T, Obukhov AG, Schaefer M, Harteneck C, Gudermann T, Schultz G. Direct activation of TRPC6 and TRPC3 channels by diacylglycerol. Nature. 2009;397:259-63.

61. Takai Y, Sasaki T, Matozaki T. Small GTP-binding proteins. Physiol Rev. 2001;1(1):153-208.

62. Tognon CE, Kirk HE, Passmore LA, Whitehead IP, Der CJ, Kay RJ. Regulation of RasGRP via a phorbol ester-responsive C1 domain. Mol Cell Biol. 1998;18(12):6995-7008.

63. Kawasaki T, Ueyama T, Lange I, Feske S, Saito N. Protein kinase C-induced phosphorylation of Orai1 regulates the intracellular Ca2+ level via the store-operated Ca2+ channel. J Biol Chem. 2010;285(33):25720-30.

64. Puchkov D, Haucke V. Greasing the synaptic vesicle cycle by membrane lipids. Trends Cell Biol. 2013;23(10):493-503.

65. Rohrbough J, Broadie K. Lipid regulation of the synaptic vesicle cycle. Nat Rev Neurosci. 2005;6(2):139-50.

66. Vasudevan EL, Jeromin A, Volpicelli-Daley L, De Camilli P, Holowka D, Baird B. The b- and c-isoforms of type I PIP5K regulate distinct stages of Ca2+ signaling in mast cells. J Cell Sci 122 (2009) 2567–2574. 2009;122:2567-74.

67. Giridharan SS, Cai B, Vitale N, Naslavsky N, Caplan S. Cooperation of MICAL-L1, syndapin2, and phosphatidic acid in tubular recycling endosome biogenesis. Mol Biol Cell. 2013;24(11):1776-90, S1-15.

68. Burger KN, Demel RA, Schmid SL, de Kruijff B. Dynamin is membrane-active: lipid insertion is induced by phosphoinositides and phosphatidic acid. Biochemistry. 2000;39(40):12485-93.

69. Takei K, Haucke V, Slepnev V, Farsad K, Salazar M, Chen H, et al. Generation of coated intermediates of clathrin-mediated endocytosis on protein-free liposomes. Cell. 1998;94(1):131-41.

70. Rainero E, Caswell PT, Muller PA, Grindlay J, McCaffrey MW, Zhang Q, et al. Diacylglycerol kinase alpha controls RCP-dependent integrin trafficking to promote invasive migration. J Cell Biol. 2012;196(2):277-95.

71. Shulga YV, Topham MK, Epand RM. Substrate specificity of diacylglycerol kinase-epsilon and the phosphatidylinositol cycle. FEBS Lett. 2011;585(24):4025-8.

72. Kearns BG, McGee TP, Mayinger P, Gedvilaite A, Phillips SE, Kagiwada S, et al. Essential role for diacylglycerol in protein transport from the yeast Golgi complex. Nature. 1997;387(6628):101-5.

73. Shemesh T, Luini A, Malhotra V, Burger KN, Kozlov MM. Prefission constriction of Golgi tubular carriers driven by local lipid metabolism: a theoretical model. Biophys J. 2003;85(6):3813-27.

74. Kooijman EE, Chupin V, de Kruijff B, Burger KN. Modulation of membrane curvature by phosphatidic acid and lysophosphatidic acid. Traffic. 2003;4(3):162-74.

75. Szule J, Fuller, N., Rand, R. The effects of acyl chain length and saturation of diacylglycerols and phosphatidylcholines on membrane monolayer curvature. Biophys J. 2002;83:977-84.

76. Burger KN. Greasing membrane fusion and fission machineries. Traffic. 2000;1(8):605-13.

77. Liljedahl M, Maeda, Y., Colanzi, A., Ayala, I., Van Lint, J., and Malhotra, V. Protein Kinase D Regulates the Fission of Cell Surface Destined Transport Carriers from the Trans-Golgi Network. Cell. 2001;104:409-20.

78. Bai J, Pagano RE. Measurement of spontaneous transfer and transbilayer movement of BODIPY-labeled lipids in lipid vesicles. Biochemistry. 1997;36(29):8840-8.

79. Rincon E, Santos T, Avila-Flores A, Albar JP, Lalioti V, Lei C, et al. Proteomics identification of sorting nexin 27 as a diacylglycerol kinase zeta-associated protein: new diacylglycerol kinase roles in endocytic recycling. Molecular & cellular proteomics : MCP. 2007;6(6):1073-87.

80. Betz A, Ashery U, Rickmann M, Augustin I, Neher E, Sudhof TC, et al. Munc13-1 is a presynaptic phorbol ester receptor that enhances neurotransmitter release. Neuron. 1998;21(1):123-36.

81. Hutagalung AH, Novick PJ. Role of Rab GTPases in membrane traffic and cell physiology. Physiol Rev. 2011;91(1):119-49.

82. Chen Y, Lippincott-Schwartz J. Insulin triggers surface-directed trafficking of sequestered GLUT4 storage vesicles marked by Rab10. Small GTPases. 2013;4(3):193-7.

83. Sanjuán MA, Jones DR, Izquierdo M, Mérida I. Role of Diacylglycerol Kinase α in the Attenuation of Receptor Signaling. J Cell Biol. 2001;153(1):207-20.

84. Alonso R, Mazzeo C, Rodriguez MC, Marsh M, Fraile-Ramos A, Calvo V, et al. Diacylglycerol kinase alpha regulates the formation and polarisation of mature multivesicular

bodies involved in the secretion of Fas ligand-containing exosomes in T lymphocytes. Cell death and differentiation. 2011;18(7):1161-73.

85. Fallman M, Lew DP, Stendahl O, Andersson T. Receptor-mediated phagocytosis in human neutrophils is associated with increased formation of inositol phosphates and diacylglycerol. Elevation in cytosolic free calcium and formation of inositol phosphates can be dissociated from accumulation of diacylglycerol. The Journal of clinical investigation. 1989;84(3):886-91.

86. Topham MK, Bunting M, Zimmerman GA, McIntyre TM, Blackshear PJ, Prescott SM. Protein kinase C regulates the nuclear localization of diacylglycerol kinase-zeta. Nature. 1998;394(6694):697-700.

87. Okada M, Hozumi Y, Iwazaki K, Misaki K, Yanagida M, Araki Y, et al. DGKzeta is involved in LPS-activated phagocytosis through IQGAP1/Rac1 pathway. Biochem Biophys Res Commun. 2012;420(2):479-84.

88. Abramovici H, Gee SH. Morphological changes and spatial regulation of diacylglycerol kinase-zeta, syntrophins, and Rac1 during myoblast fusion. Cell motility and the cytoskeleton. 2007;64(7):549-67.

89. Sholl, DA. Dendritic organization in the neurons of the visual and motor cortices of the cat. J. Anat. 1953;87:387–406.